# Preparation and Characterization of Ni-Al and Co-Al Layered Double Hydroxide by Reduction-Oxidation Method

Pallavi G., Vidyashree B. K. and Ramesh T. N.*
*Department of Studies and Research in Chemistry*
*University College of Science, Tumkur University, Tumkakuru 572103, India*

***Abstract***

*Layered double hydroxides have been extensively used as electrode materials, adsorbents and precursors for catalysts. In this work, a simple preparative method was adopted, and its influence on the crystallinity and band gap values was investigated. Cobalt-aluminium and nickel-aluminium based layered double hydroxides (0.75:0.25/0.667:0.333) were prepared using the reduction-oxidation method. $Ni^{2+}$/$Co^{2+}$ cations were reduced to metallic cobalt/nickel using sodium borohydride in the presence of trivalent aluminium ions and sodium carbonate solution at 28- 30 °C to prepare layered double hydroxides (LDHs). The resulting compounds were characterized using powder X-ray diffraction, infrared spectra, scanning electron microscopy and UV-visible diffuse reflectance spectra. The interplanar spacings around 7.6 Å for Co-Al LDHs (0.75/667:0.333) and Ni-Al LDHs (0.75:0.25/0.667:0.333) were observed from the powder X-ray diffraction patterns. Infrared spectral data confirm the presence of water molecules and carbonate ions in the interplanar region. Co-Al (0.75:0.25/0.667:0.333) LDH and Ni-Al (0.75:0.25/0.667:0.333) LDHs exhibit band gaps in the range of 2 to 5.4 eV, indicating that the compounds exhibit semiconducting to insulating behaviour. Scanning electron microscopic data shows irregular morphologies with particle sizes in the micrometer range for both Co-Al (0.75:0.25/0.667:0.333) LDH and Ni-Al (0.75:0.25/0.667:0.333) LDH samples, respectively.*

***Keywords:*** *Cobalt-aluminium based layered double hydroxide, Nickel-aluminium based layered double hydroxide, Layered compound, Band gap, Morphology.*

## 1. Introduction

Anionic clays called layered double hydroxides (LDHs) derive their structure from mineral brucite, in which the fraction of divalent cations is replaced by trivalent cations, to create positively charged sheets [1]. The interlayer regions of LDHs contain negatively charged ions and water molecules to counteract the positive charge and ensure stability [2]. The general formula for layered double hydroxides is represented by $[M^{(II)}_{1-x}M^{(III)}_{x}(OH)_2]^{x+}(A^{n-})_{x/n}.yH_2O$, where 'x' ranges from 0 to 0.33 and M(II) and M(III) are divalent and trivalent metal cations, respectively [3]. LDHs have several advantages due to their low cost and diversity in their chemical composition, leading to the easy tunability of their properties. LDHs have been used as catalysts, catalyst supports, polymer composite stabilizers, reinforcement materials, hosts for drug delivery materials, and adsorbents for wastewater treatments [4-8]. Several methods have been adopted to prepare LDHs due to their chemical and thermal stability. Of all the methods, the co-precipitation method from aqueous solution is often used

* Corresponding author. Tel.: +91-0816-2260220
E-mail address: adityaramesh77@yahoo.com

Manuscript History:
Received 9 June, 2026, Revised 7 August, 2026, Accepted 12 August, 2026, Published 31 October, 2026
Copyright © 2026 UNIMAS Publisher. This is an open access article under the CC BY-NC-SA 4.0 license.
https://doi.org/10.33736/jaspe.13337.2026

e-ISSN: 2289-7771

to prepare different types of LDHs [3]. Nucleation and particle growth occur simultaneously in the precipitation method, yielding aggregation of particles with irregular shape and morphology having micrometer size. To overcome this, several alternative methods, including microwave irradiation, ultrasound and nucleation and aging phases, have been reported [9-15].

The thermal decomposition of LDHs leads to the formation of mixed oxides exhibiting higher degree of basicity compared to the oxide anions. Intercalation of acidic anions into the interlayers of LDHs results in acid-base characteristics [16]. Calcined mixed oxides obtained from LDHs, upon aging in anion-containing solutions, result in the reconstruction of the structure of LDHs and the phenomena are called the memory effect [15,16]. LDHs have better anion exchange capacities (AEC) than those of cationic clays [17-18].

It is a challenge to prepare crystalline LDHs with uniform particle size and shape due to their technological applications. A novel reduction-oxidation method has been reported to prepare Ni-Al LDH [12]. In this work, reduction-oxidation method was used to prepare Co-Al LDH (0.75:0.25/0.667:0.333), Ni-Al LDH (0.75:0.25/0.667:0.333) samples at 28-30 °C and to age the obtained slurry/precipitate for 1 h and 48 h respectively in their mother liquor. The type and the composition of LDHs affect the band gap and in this report, band gap studies were carried out for Co-Al LDH (0.75:0.25/0.667:0.333) and Ni-Al LDH (0.75:0.25/0.667:0.333) samples at 28-30 °C and aged for 1 h and 48 h respectively.

## 2. Materials and methods

### 2.1. Chemicals

Nickel chloride hexahydrate, aluminium nitrate nonahydrate, sodium borohydride, sodium carbonate, and cobaltous nitrate hexahydrate were used. All the reagents were obtained from SD Fine Chemicals, Private Limited, India, and used without purification.

### 2.2. Preparation of Co-Al LDH and Ni-Al LDH samples

The preparative procedure reported by Quanyao Liu et al. has been adopted to prepare Co-Al LDH and Ni-Al LDHs [12]. To prepare Co-Al LDH (0.75:0.25), 0.5458 g of cobalt nitrate hexahydrate was dissolved in 50 mL of distilled water and 0.2344 g aluminium nitrate nonahydrate was dissolved in 50 mL of distilled water separately; these two solutions were mixed to prepare 100 mL of solution-A [$Co^{2+}$:$Al^{3+}$ molar ratio of 3:1([$Co^{(2+)}$]+[$Al^{(3+)}$]=1M]. Solution B is obtained by dissolving 0.0756 g of sodium borohydride in 20 mL of distilled water ($NaBH_4$ = 0.1 M). Solutions A and B were mixed and stirred quickly for a few minutes. Later, 0.1 M sodium carbonate solution (50 mL) is added [($Na_2CO_3$)/[Co(II)]+[Al(III)]=2] to it to obtain Co-Al LDH (0.75:0.25) at 28-30 °C. The slurry obtained was divided into two parts, first part of it was aged for 1 h and second part was aged for 48 h at 28-30 °C separately in mother liquor. Then the obtained products were filtered, washed with distilled water and dried at 28-30 °C.

Two more Co-Al LDH (0.6667:0.333) samples with $Co^{2+}$:$Al^{3+}$ mole ratio of (2:1) were also prepared by following the above method at 28-30 C and ageing for 1 h and 48 h separately. The second set of LDHs, i.e Ni-Al LDHs having $Co^{2+}$:$Al^{3+}$ mole ratios of 3:4 and 2:1 were prepared by adopting the above procedure at 28-30 °C and aged for 1 h and 48 h separately. The details of reagents used to prepare Co-Al (0.75:0.25/0.667:0.333) LDH and Ni-Al (0.75:0.25/0.667:0.333) samples are given in Table 1.

## 2.3. Characterization techniques

The samples were characterized using different techniques. To determine the structure of the samples, a Bruker D8 advanced diffractometer (Cu Kα source λ=1.5418 Å) (scan rate 4°min$^{-1}$; steps: 0.02; scan range: 10-80°) was used to record powder X-ray diffraction (pXRD) data. UV-visible DRS (UV-Vis-DRS) spectral data were measured in absorbance and reflectance modes in the range of 200-1000 nm [(UV Vis Spectroscopy JASCO (V-670 PC)]. Infrared spectra were recorded using a Thermo Nicolet iS50 with an inbuilt ATR spectrometer (Thermo Fisher Scientific, USA) to identify the characteristic functional groups present in the samples. The morphology and elemental data of the samples were collected using a scanning electron microscope (SEM) (SEM-EDAX: Jeol 6390LA/OXFORD X-MaxN, accelerating voltage: 0.5 to 30 kV) and energy dispersive X-ray analysis (EDXA).

Table 1. The quantities of reagents used to prepare Co-Al (0.75:0.25/0.667:0.333) LDH and Ni-Al (0.75:0.25/0.667:0.333) samples

| Sl. No. | LDH | Weight of the compounds taken (g)/molarity of the solution/s | | | | |
|---|---|---|---|---|---|---|
| | | Cobaltous nitrate hexahydrate | Nickel nitrate hexahydrate | Aluminium nitrate nonahydrate | Sodium carbonate | Sodium borohydride |
| 1 | $Co_{0.75}Al_{0.25}$ LDH at 28-30 °C and aged for 1 h | 0.5458 g (0.0375 M) | - | 0.2344 g (0.0125 M) | 0.5299 g (0.1 M) | 0.0756 g (0.1 M) |
| 2 | $Co_{0.67}Al_{0.33}$ LDH at 28-30 °C and aged for 1 h | 9.701 g (0.0335 M) | - | 0.3122 g (0.0166 M) | 1.0598 g (0. 2M) | 0.0756 g (0.1 M) |
| 3 | $Co_{0.75}Al_{0.25}$ LDH at 28-30 °C and aged for 48 h | 0.5458 g (0.0375 M) | - | 0.2344 g (0.0125 M) | 0.5299 g (0.1 M) | 0.0756 g (0.1 M) |
| 4 | $Co_{0.67}Al_{0.33}$ LDH at 28-30 °C and aged for 48 h | 9.701g (0.0335 M) | - | 0.3122 g (0.0166 M) | 1.0598 g (0. 2M) | 0.0756 g (0.1 M) |
| 5 | $Ni_{0.75}Al_{0.25}$ LDH at 28-30 °C and aged for 1 h | - | 0.4456 g (0.0375 M) | 0.2344 g (0.0125 M) | 0.5299 g (0.1 M) | 0.0756 g (0.1 M) |
| 6 | $Ni_{0.67}Al_{0.33}$ LDH at 28-30 °C and aged for 1 h | - | 0.3961 g (0.0333 M) | 0.3122 g (0.0166 M) | 1.0598 g (0. 2M) | 0.0756 g (0.1 M) |
| 7 | $Ni_{0.75}Al_{0.25}$ LDH at 28-30 °C and aged for 48 | - | 0.4456 g (0.0375 M) | 0.2344 g (0.0125 M) | 0.5299 g (0.1 M) | 0.0756 g (0.1 M) |
| 8 | $Ni_{0.67}Al_{0.33}$ LDH at 28-30 °C and aged for 48 h | - | 0.3961 g (0.0333 M) | 0.3122 g (0.0166 M) | 1.0598 g (0. 2M) | 0.0756 g (0.1 M) |

## 3. Results and discussion

### 3.1. XRD patterns

In the procedure used to prepare Co-Al LDH (0.75:0.25/0.667:0.333) and Ni-Al LDH (0.75:0.25/0.667:0.333) samples, Quanyao Liu et al. proposed the following reaction steps [12]:

$2M^{2+} + BH_4^- + 4H_2O \rightarrow 2M + B(OH)_4^- + 2H_2 + 4H^+$ – step-1 ($M^{2+} = Co^{2+}/Ni^{2+}$) – (1)
$2M + O_2 + 2H_2O \rightarrow 2M(OH)_2$ – (2)
$M'^{3+} + 4OH^- \rightarrow M'(OH)_4^-$ – (3) ($M'^{3+} = Al^{3+}$)
$6M(OH)_2 + 2M'(OH)_4^- + CO_3^{2-} + mH_2O \rightarrow [M_6M'_2(OH)_{16}]CO_3.mH_2O + 4OH^-$ – (4) [12].

On mixing metal salts solution ($Co^{2+}/Ni^{2+}$ with $Al^{3+}$) with sodium borohydride ($NaBH_4$), metallic cobalt/nickel is formed (step-1). The obtained metallic nuclei (cobalt/nickel) are oxidized to their respective metal hydroxides [$Ni(OH)_2/Co(OH)_2$] using the trace quantities of dissolved oxygen present in the solution (step-2). At the same time, $Al^{3+}$ ions are converted to aluminate complex anion $[Al(OH)_4]^-$ in alkali pH (step-3). In step-4, the reactions between metal hydroxide and aluminate ion [$6M(OH)_2 + 2Al(OH)_4^-$] in the presence of carbonate ion lead to the formation of M-Al LDH (M = $Co^{2+}/Ni^{2+}$) [12].

Figure 1(a-d) shows the powder XRD patterns of Co-Al LDH samples having different Co:Al mole ratio (0.75:0.25/0.67:0.33) obtained at 28-30 ° C and aged for 1 h and 48 h respectively.

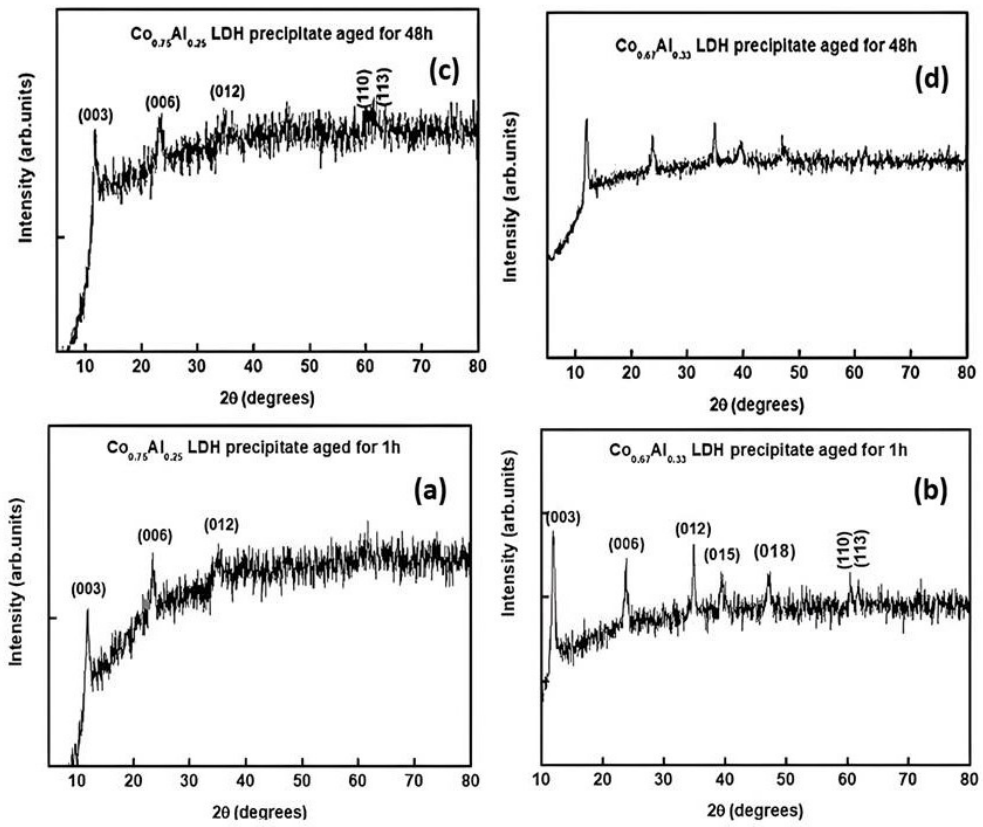



Figure 1. Powder XRD patterns of a) $Co_{0.75}Al_{0.25}$ LDH and b) $Co_{0.67}Al_{0.33}$ LDH obtained at 28-30 °C, aged for 1 h; c) $Co_{0.75}Al_{0.25}$ LDH and d) $Co_{0.67}Al_{0.33}$ LDH samples obtained at 28-30 °C and aged for 48 h separately.

For $Co_{0.75}Al_{0.25}$ LDH sample aged at 28-30 °C for 1 h, the first two peaks in the powder X-ray diffraction (XRD) patterns were observed at 2θ = 11.76° and 2θ = 23.08° Å having d spacings of 7.51 Å and 3.85 Å. The first two reflections at 2θ = 11.74° and 2θ = 23.96° Å having d spacings of 7.53 Å and 3.71 Å was observed for $Co_{0.67}Al_{0.33}$ LDH sample aged for 1 h at 28-30 °C. The reflections for both the samples could be indexed to (003) and (006) planes indicating that they have layered structure (Figures 1a and 1b).

Figure 1(c,d) shows the powder XRD patterns of Co-Al LDH samples having different Co:Al mole ratio (0.75:0.25/0.67:0.33) obtained at 28-30 °C and aged for 48 h separately. While the first two peaks for $Co_{0.75}Al_{0.25}$ LDH sample aged for 48 h at 28-30 °C was observed at 2θ = 11.66° and 2θ = 23.13° Å having d spacings of 7.58 Å and 3.84 Å and the first two peaks at 2θ = 11.86° and 2θ = 23.57° Å having d spacings of 7.45 Å and 3.77 Å for $Co_{0.67}Al_{0.33}$ LDH sample aged for 48 h at 28-30 °C. Figures 1c and 1d show the reflections in the powder X-ray diffraction patterns of $Co_{0.75}Al_{0.25}$ LDH and $Co_{0.67}Al_{0.33}$ LDH samples aged for 48 h at 28-30 °C which could be indexed to hydrotalcite (JCPDS 14-191). The lattice parameters (a=b and c) for $Co_{0.75}Al_{0.25}$ LDH and $Co_{0.67}Al_{0.33}$ LDH samples were calculated using cation–cation distance in the brucite-like layer [$2d_{(110)}$)] and thickness of one brucite-like layer and one interlayer (c = $3d_{003}$). The lattice parameters for $Co_{0.75}Al_{0.25}$ LDH and $Co_{0.67}Al_{0.33}$ LDH aged at 28-30 °C for 48 h are c = 22.743 Å and 22.327 Å respectively. With decrease in the aluminium content in Co-Al LDHs, there is a marginal reduction in the d-spacing from 7.53 Å to 7.513 Å due to lower anion content.

The lattice parameter 'c' indicates that the LDHs are of 3-layer polytype (3R) [19]. The calculated lattice parameters for $Co_{0.75}Al_{0.25}$ LDH and $Co_{0.67}Al_{0.33}$ LDH samples aged for 1 h are a = 3.06 Å, c = 22.391 Å and a = 3.063 Å, c = 22.581 Å respectively.

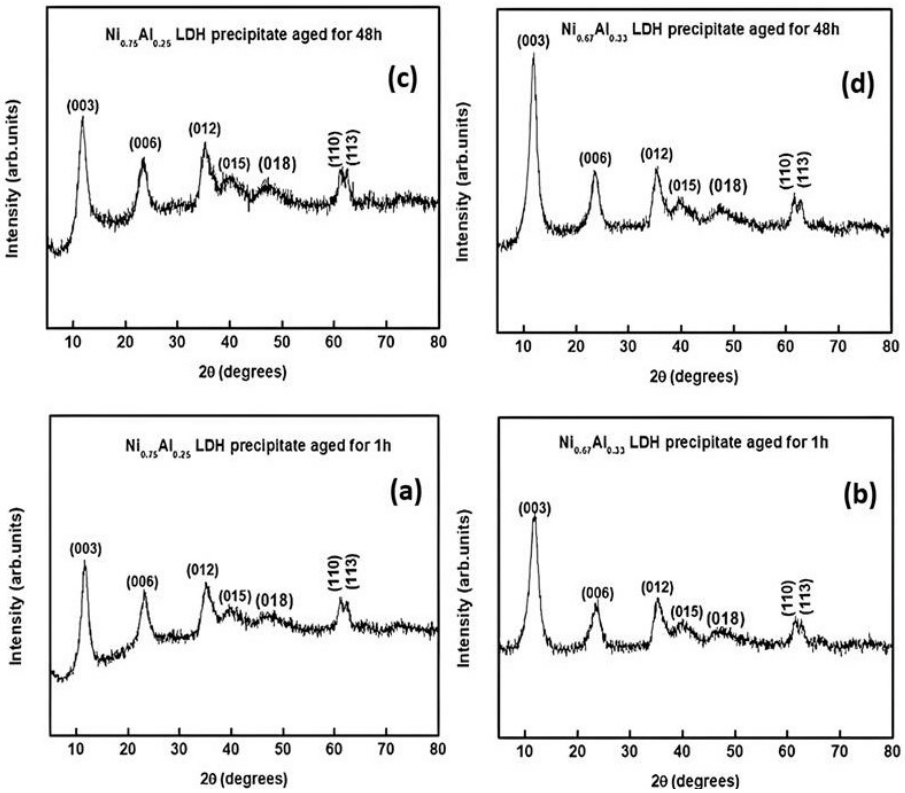



Figure 2. Powder X-ray diffraction patterns of a) $Ni_{0.75}Al_{0.25}$ LDH and b) $Ni_{0.67}Al_{0.33}$ LDH obtained at 28-30 °C, aged for 1 h; c) $Ni_{0.75}Al_{0.25}$ LDH and d) $Ni_{0.67}Al_{0.33}$ LDH samples obtained 28-30 °C and aged for 24 h separately.

Figure 2(a,b) shows the powder XRD patterns of Ni-Al LDH samples having different Ni:Al mole ratio (0.75:0.25/0.67:0.33) obtained at 28-30 °C and aged for 1 h separately and the peaks could be indexed to hydrotalcite (JCPDS 14-191). The first two lines in the powder X-ray diffraction patterns for $Ni_{0.75}Al_{0.25}$ LDH sample aged for 1 h at 28-30 °C was observed at 2θ = 11.56° and 2θ = 23.2° Å having d spacings of 7.62 Å and 3.83 Å. While the first two peaks at 2θ = 11.57° and 2θ = 23.2° Å have d spacings of 7.57 Å and 3.81 Å for $Ni_{0.67}Al_{0.33}$ LDH sample aged for 1 h at 28-30 °C. The lattice parameters for $Ni_{0.75}Al_{0.25}$ LDH and $Ni_{0.67}Al_{0.33}$ LDH samples aged for 1 h at 28-30 °C are a = 3.03 Å, c = 22.90 Å and a = 3.013 Å, c = 22.71 Å and respectively. Figure 2(c,d) shows the powder XRD patterns of Ni-Al LDH samples having different Ni:Al mole ratio (0.75:0.25/0.67:0.33) obtained at 28-30 °C and aged for 48 h separately. The first two reflections for $Ni_{0.75}Al_{0.25}$ LDH sample aged for 48 h at 28-30 °C was observed at 2θ = 11.672° and 2θ = 23.29° Å having d spacings of 7.575 Å and 3.81 Å, whereas the reflections in the pXRD patterns of $Ni_{0.67}Al_{0.33}$ LDH sample aged for 48 h at 28-30 °C were observed at 2θ = 11.765° and 2θ = 23.475° Å having d spacings of 7.515 Å and 3.78 Å respectively. The lattice parameters for $Ni_{0.75}Al_{0.25}$ LDH and $Ni_{0.67}Al_{0.33}$ LDH samples aged for 48 h at 28-30 °C are a = 3.02 Å, c = 22.725 Å and a = 3.008 Å, c = 22.545 Å and respectively [19].

The interplanar distance of Co-Al LDH and Ni-Al LDH samples depends on i) the charge density of the layer, ii) type of anion ($CO_3^{2-}$) and iii) the number of moles of water molecules present between the interlayer. The 'a' parameter changes marginally and is independent of the preparative conditions of Co-Al LDH (0.75:0.25/0.67:0.33) and Ni-Al LDH (0.75:0.25/0.67:0.33) samples.

### 3.2. Infrared spectral data

Figure 3(a,b) shows the infrared spectral data of Co-Al LDH samples having different Co:Al mole ratio (0.75:0.25/0.67:0.33) obtained at 28-30 °C and aged at 28-30 °C for 1 h separately.

Figure 3(a) shows the infrared spectral data of Co-Al LDH samples having Co:Al mole ratio (0.75:0.25) obtained at 28-30 °C and aged for 1 h separately. The broad peak observed at 3405 $cm^{-1}$ could be indexed to OH stretching vibration from the layer and water molecules. The peak observed at 1637 $cm^{-1}$for $Co_{0.75}Al_{0.25}$ LDH (Figure 3a) is due to deformation mode of vibrations of interlayer water molecules i.e. $\delta(H_2O)$. The peak at 1355 $cm^{-1}$ is assigned to the anti-symmetric stretching mode ($\nu_3$) of $CO_3^{2-}$ ion. The bending modes observed at 723 $cm^{-1}$ is assigned to $\nu_4$ mode of carbonate anion in the $Co_{0.75}Al_{0.25}$ LDH structure. The 546 $cm^{-1}$ band arise due to OH–O bond/interaction formed between the intercalated water and $CO_3^{2-}$ ion of $Co_{0.75}Al_{0.25}$ LDH sample aged for 1 h (see Figure 3a).

The peak observed at 3558 $cm^{-1}$ is indexed to OH stretching vibrations from the layer and water molecules. Bending modes of vibrations of OH groups arise due to the presence of interlayer water molecules and are observed in the range of 1600 $cm^{-1}$ to 1700 $cm^{-1}$. The peak observed at 1632 $cm^{-1}$ for $Co_{0.67}Al_{0.33}$ LDH is due to H-O-H deformation mode of vibrations from interlayer water molecules i.e. $\delta(H_2O)$. The band observed at 1348 $cm^{-1}$ can be attributed to the anti-symmetric stretching mode ($\nu_3$) of $CO_3^{2-}$ group. The out-of-plane bending mode $\nu_2$ varies from 862 to 892 $cm^{-1}$ depending on the nature of the cation. The $\nu_2$ bending mode is observed at 770 $cm^{-1}$ and 691 $cm^{-1}$ is assigned to $\nu_4$ mode of carbonate anion in the $Co_{0.67}Al_{0.33}$ LDH structure. The 551 $cm^{-1}$ band is distinct for the structure of layered double hydroxide and could arise due to OH–O bond/interaction formed between the intercalated water and $CO_3^{2-}$ ion [see Figure 3(b)] [20-21].

Figure 3(c,d) shows the infrared spectral data of Co-Al LDH samples having different Co:Al mole ratio (0.75:0.25/0.67:0.33) obtained at 28-30 °C and aged for 48 h separately. The peak assignments for the above samples are given in Table 2. Figure 4(a,b) shows the infrared spectral data of Ni-Al LDH samples having Ni:Al mole ratio (0.75:0.25/0.67:0.33) obtained at 28-30 °C and aged for 1 h separately. Figure 4(c,d) shows the infrared spectral data of Ni-Al LDH samples having Ni:Al mole ratio (0.75:0.25/0.67:0.33) obtained at 28-30 °C and aged for 48 h separately. The assignment of the peaks observed for the above samples is given in Table 2.

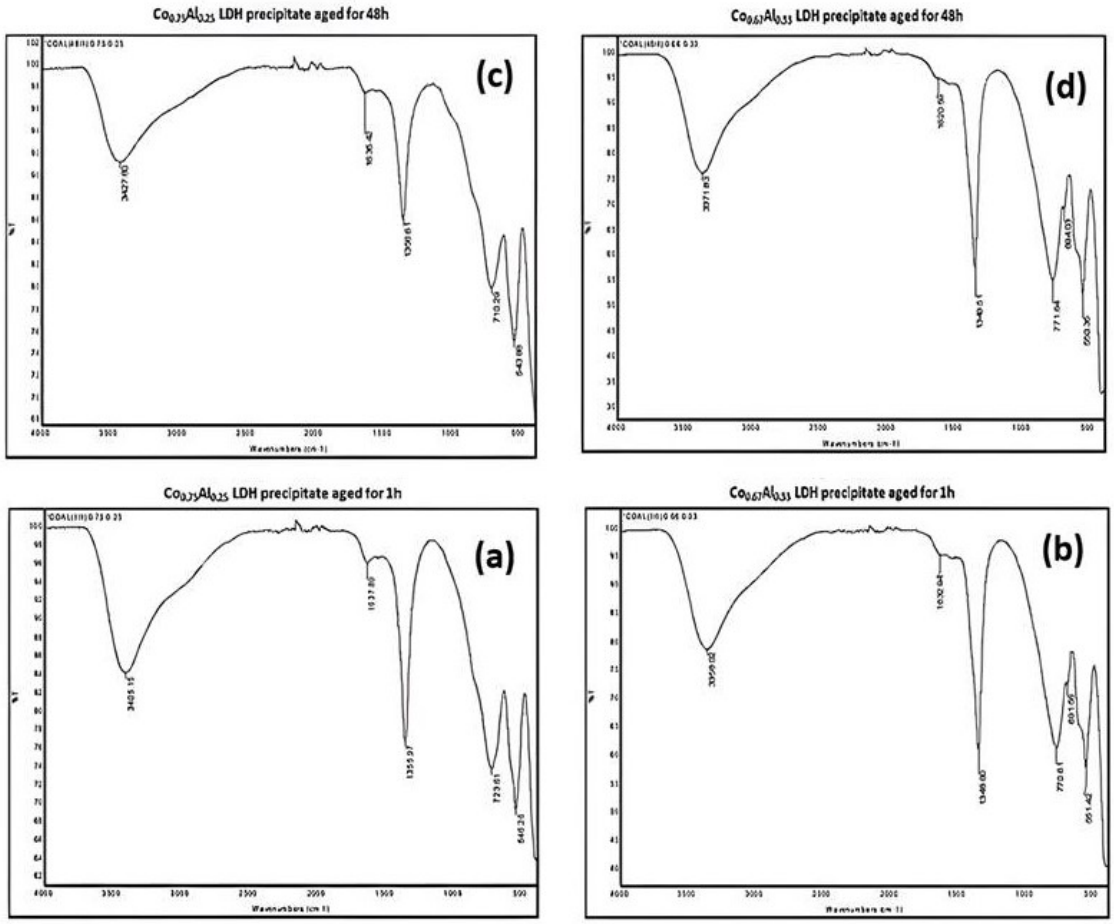



Figure 3. Infrared spectra of a) $Co_{0.75}Al_{0.25}$ LDH and b) $Co_{0.67}Al_{0.33}$ LDH obtained at 28-30 °C, aged for 1 h; c) $Co_{0.75}Al_{0.25}$ LDH and d) $Co_{0.67}Al_{0.33}$ LDH samples obtained at 28-30 °C and aged for 24 h separately.

### 3.3. UV-VIS spectral data

The compounds can be categorized into conductors, semiconductors and insulators based on their electrical conductivity/band gap values. There will be no band gap for conductors, while for semiconductors and insulators, it is in the range of 1.5 to 3 eV and 3-5 eV respectively.

Generally, layered double hydroxide samples exhibit three absorption bands in the UV and visible-light regions of the electromagnetic spectrum at 28–30 (°C). The first band is observed in the range of 200 to 300 nm, the second in the range of 300 to 550 nm and the third in the range of 600 to 800 nm. The 200-300 nm bands are assigned to ligand-to-metal charge transfer (LMCT) from the O-2p orbital to M-3d($t_{2g}$) orbital and the peaks exhibited in the 300 to 800 range correspond to d-d transitions, from the $M^{2+}$ ($Co^{2+}$/$Ni^{2+}$) ions in an octahedral geometry [22,23]. Also, DFT studies have been carried out to investigate the energy and band gap in layered double hydroxides [24].

UV-visible diffused reflectance/absorption spectra were obtained for Co-Al LDH (0.75:0.25/0.67:0.33) and Ni-Al LDH (0.75:0.25/0.67:0.33) samples to study the optical property of the samples. Figure 5(a) shows the UV-visible DRS spectra of $Co_{0.75}Al_{0.25}$ LDH sample recorded in absorbance mode, and the band gaps for the various peaks are observed at 4.81 eV, 3.5 eV (weak),

2.37 eV respectively. Also Figure 5(a′) gives the Tauc plot of $Co_{0.75}Al_{0.25}$ LDH prepared at 28-30 °C for 1 h from which the calculated band gaps are observed at 1.69 eV and 2.0 eV respectively.

From the UV-visible DRS absorbance plot, the calculated band gap (eV) values for $Co_{0.67}Al_{0.33}$ LDH prepared at 28-30 °C for 1 h is 4.88 eV (Figure 5b). Along with these, additional values of band gaps at 2.40 eV and 2.07 eV were observed, indicating that the intrinsic property is insulating in nature. Based on the Tauc plot, the observed band gaps for the above sample are 1.75 eV and 2.07 eV respectively (see Figure 5b′).

Table 2: Assignment of peaks observed for Co-Al LDH (0.75:0.25; 0.667:0.333) and Ni-Al LDH (0.75:0.25; 0.667:0.333) samples prepared at 28-30 °C and aged for 1h and 48 h respectively

| **Sample** | **Assignment of peaks (wave number, $cm^{-1}$)** | | | | |
|---|---|---|---|---|---|
| | **OH stretch due to layer OH and interlayer $H_2O$ molecules** | **Deformation mode $\delta(H_2O)$** | **anti-symmetric stretching mode of $CO_3^{2-}$ ion** | **bending mode** | **OH–O bond/interaction formed between the intercalated water and $CO_3^{2-}$ ion** |
| $Co_{0.75}Al_{0.25}$ LDH at 28-30 °C and aged for 1 h | 3405 | 1637 | 1355 | 723 | 546 |
| $Co_{0.67}Al_{0.33}$ LDH at 28-30 °C and aged for 1 h | 3558 | 1632 | 1348 | 770, 691 | 551 |
| $Co_{0.75}Al_{0.25}$ LDH at 28-30 °C and aged for 48 h | 3427 | 1635 | 1356 | 710 | 543 |
| $Co_{0.67}Al_{0.33}$ LDH at 28-30 °C and aged for 48 h | 3371 | 1620 | 1349 | 694 | 550 |
| $Ni_{0.75}Al_{0.25}$ LDH at 28-30 °C and aged for 1 h | 3403 | 1633 | 1358 | 703 | 551 |
| $Ni_{0.67}Al_{0.33}$ LDH at 28-30 °C and aged for 1 h | 3332 | 1632 | 1348 | 764, 691 | 559 |
| $Ni_{0.75}Al_{0.25}$ LDH at 28-30 °C and aged for 48 | 3380 | 1635 | 1357 | 721 | 554 |
| $Ni_{0.67}Al_{0.33}$ LDH at 28-30 °C and aged for 48 h | 3345 | 1630 | 1348 | 784, 689 | 560 |

The band gap (eV) values of $Co_{0.75}Al_{0.25}$ LDH prepared at 28-30 °C for 48 h is 4.71 eV. In addition to the above, we observe additional band gap values at 3.39 eV (weak) and 2.41 eV (see Figure 6a). Based on the Tauc plot, we observe band gaps for the above sample at 1.63 eV and 1.97 eV respectively (Figure 6a′).

The band gap (eV) values of $Co_{0.67}Al_{0.33}$ LDH prepared at 28-30 °C for 48 h is 5.04 eV. Also, we observe an additional band gap at 2.36 eV (see Figure 6b). Based on the Tauc plot, the observed band gaps for the above sample at 1.77 eV and 2.10 eV, respectively (Figure 6b′).

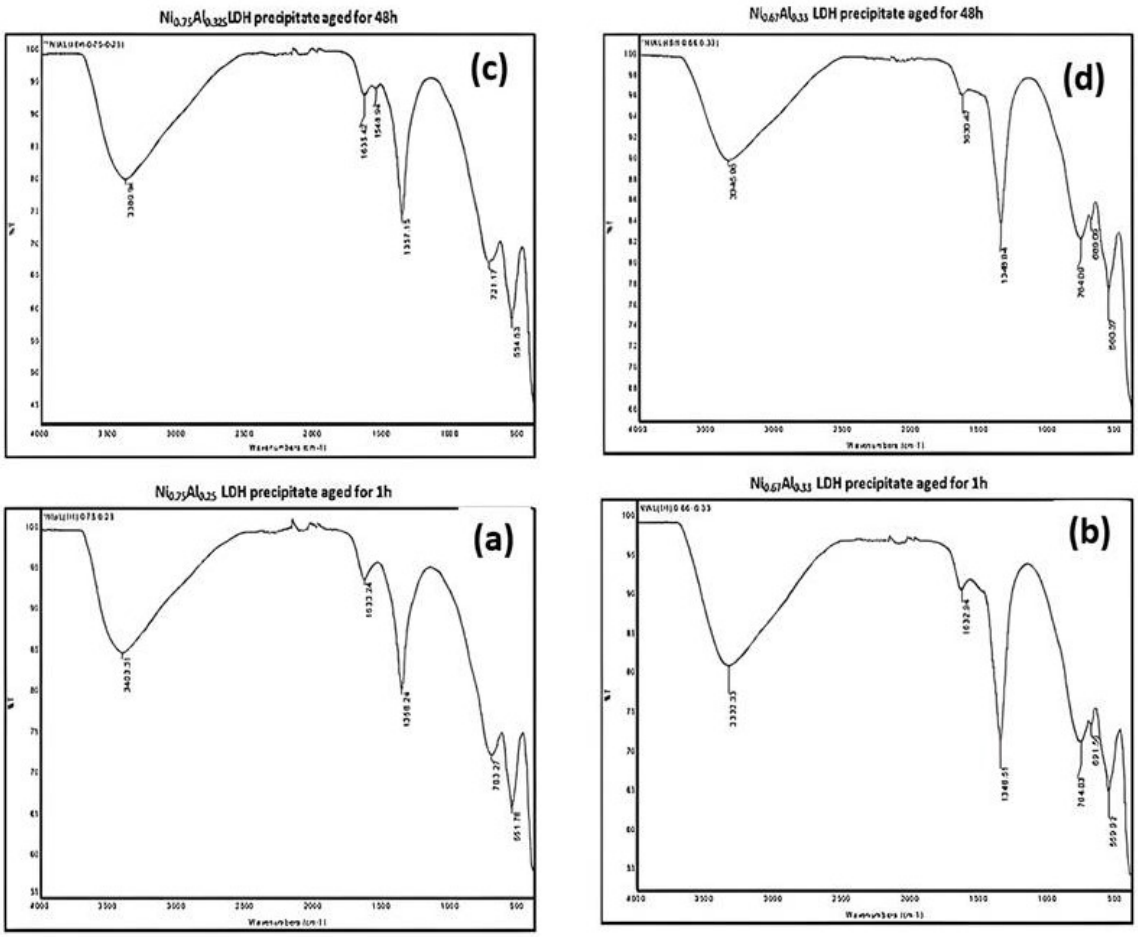



Figure 4. Infrared spectra of of a) $Ni_{0.75}Al_{0.25}$ LDH and b) $Ni_{0.67}Al_{0.33}$ LDH obtained at 28-30 °C and aged for 1 h; c) $Ni_{0.75}Al_{0.25}$ LDH and d) $Ni_{0.67}Al_{0.33}$ LDH samples obtained at 28-30 °C and aged for 24 h separately.

The band gap (eV) value obtained from the absorbance data of UV-visible DRS of $Ni_{0.75}Al_{0.25}$ LDH prepared at 28-30 °C for 1 h is 5.04 eV (Figure 7a). In addition to the above, the observed additional band gap values are 3.32 eV (weak) and 1.90 eV. Based on the Tauc plot, the band gap for the above sample is 1.56 eV (Figure 7a′).

From the absorbance of UV-visible DRS data, the calculated band gap (eV) value of $Ni_{0.67}Al_{0.33}$ LDH prepared at 28-30 °C for 1 h is 5.54 eV. Additional band gap values are observed at 3.27 eV (weak) and 1.93 eV (Figure 7b). Based on the Tauc plot, the band gap values for the above sample are observed at 1.77 eV and 2.10 eV respectively (Figure 7b′).

The band gap (eV) values of $Ni_{0.75}Al_{0.25}$ LDH prepared at 28-30 °C for 48 hr is 5.37 eV (Figure 8a). In addition to the above, we observe additional band gap values at 3.25 eV (weak) and 1.90 eV. Based on the Tauc plot, we observe a band gap for the above sample at 1.56 eV (Figure 8a').

Based on the UV-visible DRS spectra, the band gap (eV) value of $Ni_{0.67}Al_{0.33}$ LDH prepared at 28-30 °C for 48 h is 5.21 eV (Figure 8b). In addition to the above, additional band gap values of 3.33 eV (weak) and 1.97 eV were observed. Based on the Tauc plot, the band gap for the above sample is 1.45 eV (Figure 8b′). Due to the low band gap values observed for both CoAl-LDH and NiAl-LDH samples, they are semiconducting in nature.

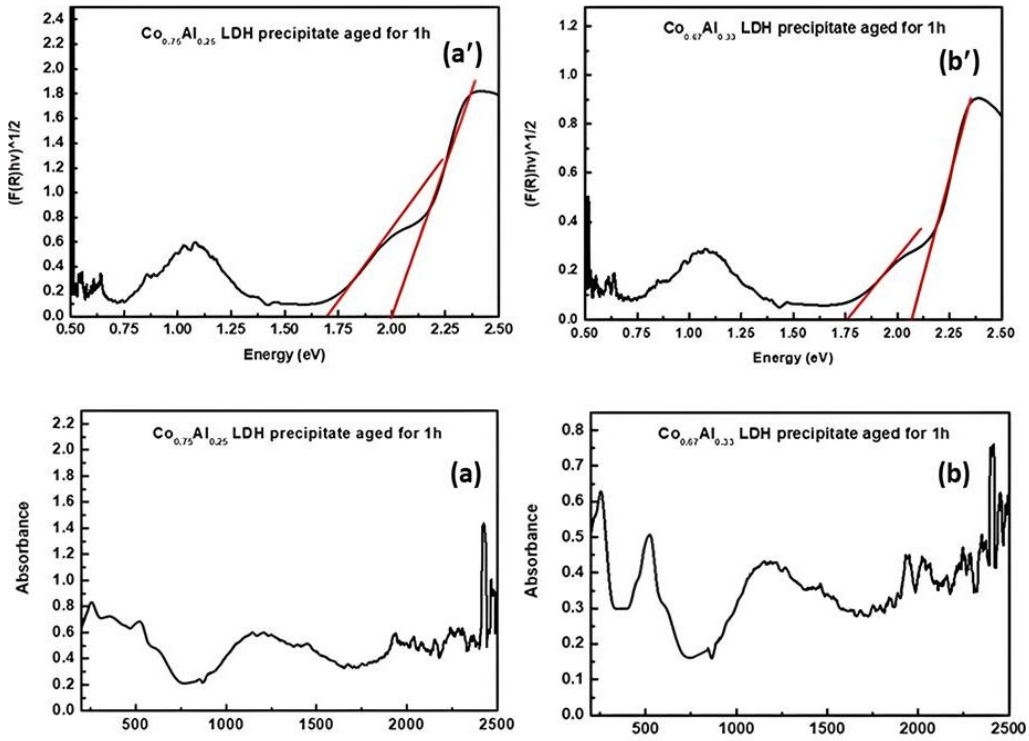



Figure 5. UV-visible DRS in absorbance mode and Tauc plot of a)-a′) $Co_{0.75}Al_{0.25}$ LDH b)-b′) and $Co_{0.67}Al_{0.33}$ LDH samples obtained at 28-30 °C and aged for 1 h separately.

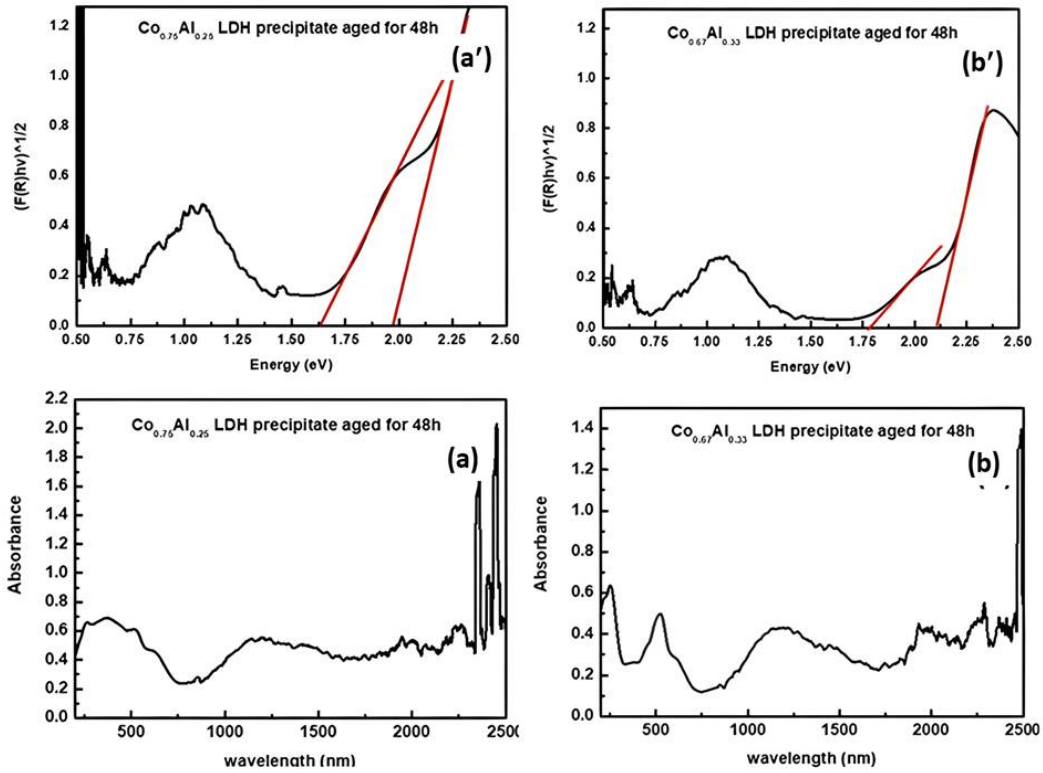



Figure 6. UV-visible DRS in absorbance mode and Tauc plot of a)-a′) $Co_{0.75}Al_{0.25}$ LDH and b)-b′) $Co_{0.67}Al_{0.33}$ LDH samples obtained at 28-30 °C and aged for 48 h separately.

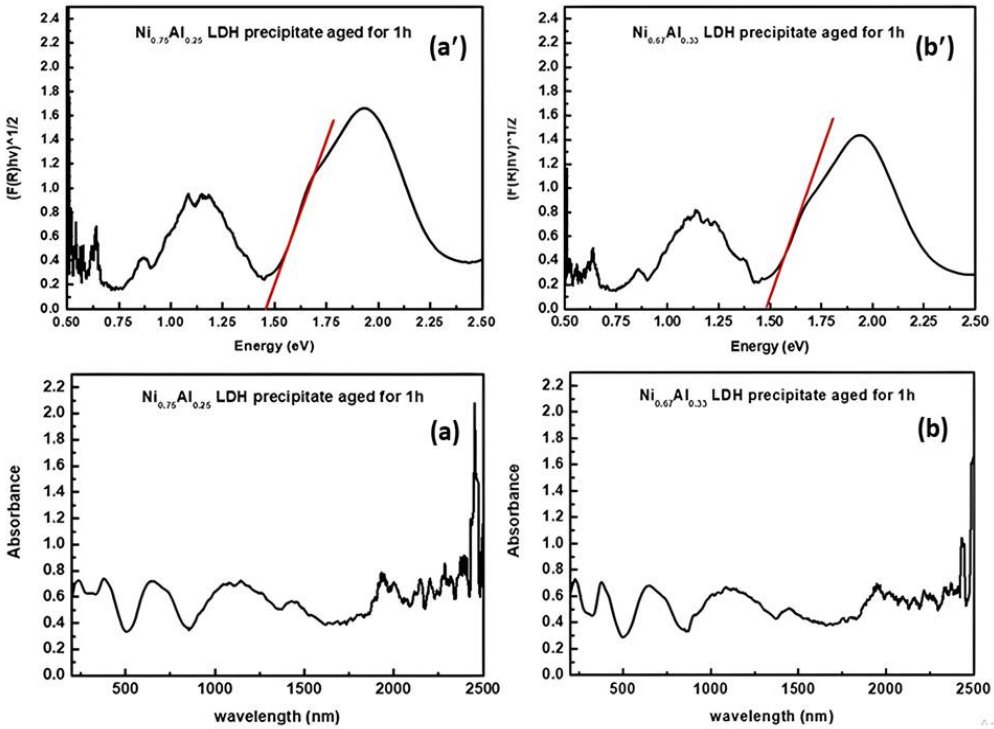



Figure 7. UV-visible DRS in absorbance mode and Tauc plot of a)-a′) b)-b′) $Ni_{0.75}Al_{0.25}$ LDH and $Ni_{0.67}Al_{0.33}$ LDH samples obtained at 28-30 °C and aged for 1 h separately.

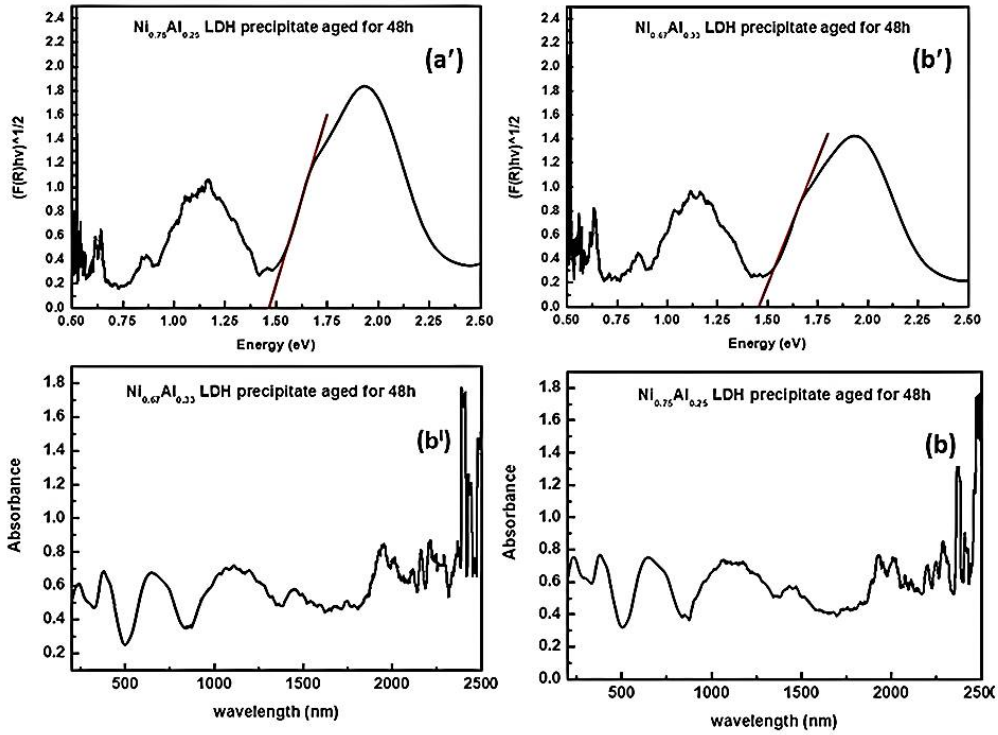



Figure 8. UV-visible DRS in absorbance mode and Tauc plot of a)-a′) $Ni_{0.67}Al_{0.33}$ LDH and b)-b′) $Ni_{0.75}Al_{0.25}$ LDH samples obtained at 28-30 °C and aged for 48 h separately.

The band gap (eV) values for Ni-Al LDH (0.75:0.25/0.66:0.33) samples prepared at 28-30 °C and aged for 1 h/48 h are in the range of 1.4 to 2.05 eV indicating that Ni-Al LDHS (0.72:0.25/0.667:0.333) also exhibit a band gap in the range of semiconductors.

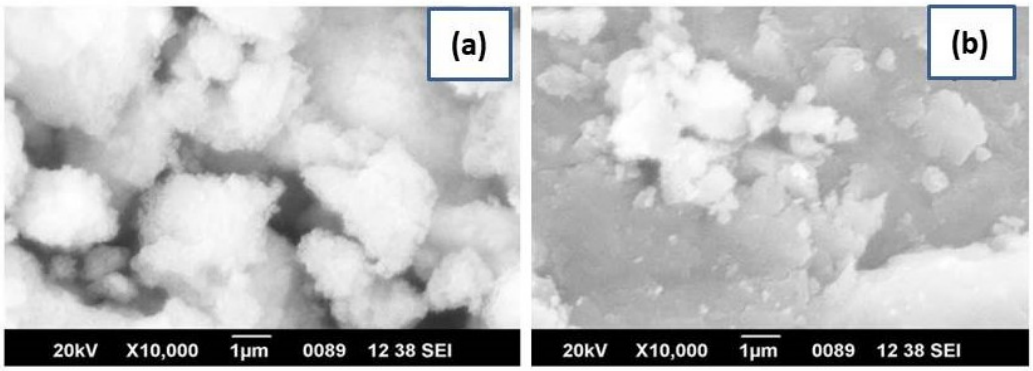



Figure 9. Scanning electron micrographs of a) $Co_{0.75}Al_{0.25}$ LDH and b) $Co_{0.67}Al_{0.33}$ LDH samples obtained at 28-30 °C and aged for 1 h separately.

Figure 9 shows the scanning electron micrographs of $Co_{0.75}Al_{0.25}$ LDH and $Co_{0.67}Al_{0.33}$ LDH samples obtained at 28-30 °C and aged for 1 h separately. They exhibit irregular morphologies, and the particle size is in the micrometer range.

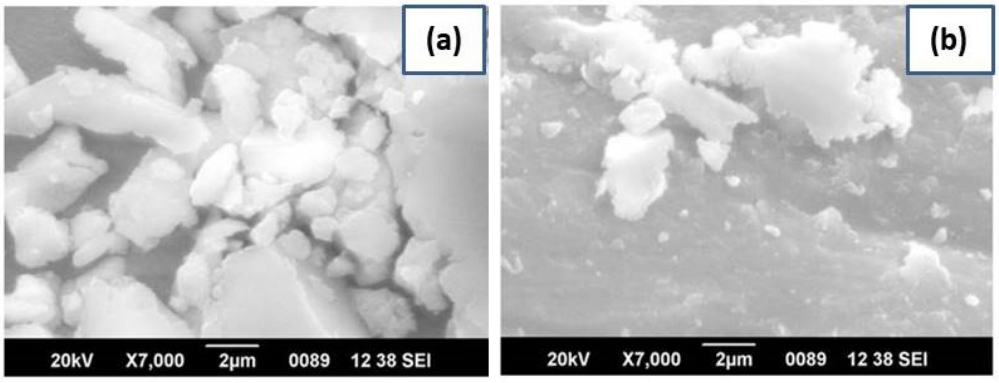



Figure 10. Scanning electron micrographs of a) $Ni_{0.75}Al_{0.25}$ LDH and b) $Ni_{0.67}Al_{0.33}$ LDH samples obtained at 28-30 °C and aged for 1 h separately.

Figure 10 shows the scanning electron micrographs of a) $Ni_{0.75}Al_{0.25}$ LDH and b) $Ni_{0.67}Al_{0.33}$ LDH samples obtained at 28-30 °C and aged for 1 h separately. They also exhibit irregular morphologies with micrometer-range particles.

From the above data, it is indicated that Co-Al LDHs have a slightly lower band gap compared to NiAl-LDHs. The LDH samples (Co-Al LDH/Ni-Al LDH having different mole ratios: 0.67:0.33/0.75:0.25) exhibit absorption peaks ranging from the UV region to the visible region of the electromagnetic spectrum. Co-Al LDH and Ni-Al LDHs have been used as photocatalysts in the degradation of toxic organic reagents/dyes [25-27]. The above data can provide insight into the variation in band gap depending on the type of the LDHs and can be used for their potential applications in photocatalysis.

## 4. Conclusions

CoAl-LDHs (0.75:0.25/0.667:0.333) and NiAl-LDHs (0.75:0.25/0.667:0.333) with better crystallinity were prepared by reduction-oxidation method. The advantage of this technique is that it will lead to the formation of crystalline samples. The preparative method can be adopted to synthesize different types of layered double hydroxides having diverse combinations of divalent metal ions with aluminium ions provided the divalent metal ions exhibit redox behavior. The LDH samples Co-Al LDH and Ni-Al LDH (0.75:0.25/0.667:0.333)] having different mole ratios exhibit absorption peaks ranging from the UV region to the visible region of the electromagnetic spectrum. Therefore, Co-Al and Ni-Al LDHs have potential applications in the wide spectral range (UV-visible) for photocatalytic applications.

## Acknowledgements

The authors would like to express their sincere appreciation to all individuals and Tumkur University for support and facilities throughout this study.

## Conflict of Interest

The authors declare no conflict of interest.

## References

[1] He, J., Wei, M., Li, B., Kang, Y., Evans, D. G., & Duan, X. (2006). Preparation of layered double hydroxides. In: Duan, X., Evans, D. G. (eds) *Layered Double Hydroxides. Structure and Bonding*, Vol *119*, 89-119, Springer, Berlin, Heidelberg. https://doi.org/10.1007/b100426

[2] Mishra, G., Dash, B., & Pandey, S. (2017). Layered double hydroxides: A brief review from fundamentals to application as evolving biomaterials. *Applied Clay Science*, *153*, 172–186. https://doi.org/10.1016/j.clay.2017.12.021

[3] Altalhi, A. A., Mohamed, E. A., & Negm, N. A. (2024). Recent advances in layered double hydroxide (LDH)-based materials: fabrication, modification strategies, characterization, promising environmental catalytic applications, and prospective aspects. *Energy Advances*, 3(9), 2136–2151. https://doi.org/10.1039/d4ya00272e

[4] Mohapi, M., Sefadi, J. S., Mochane, M. J., Magagula, S. I., & Lebelo, K. (2020). Effect of LDHs and other clays on polymer composite in adsorptive removal of contaminants: A review. *Crystals*, *10*(11), 957. https://doi.org/10.3390/cryst10110957

[5] Hadnadjev-Kostic, M., Vulic, T., Karanovic, D., Tomic, A., & Cvetkovic, D. (2025). Layered double hydroxide-based materials for wastewater treatment: Recent progress in multifunctional environmental applications. *Processes*, *13*(12), 3757. https://doi.org/10.3390/pr13123757

[6] Kumari, S., Sharma, V., Sharma, V., Soni, S., Sharma, A., Thakur, A., Kumar, S., Dhama, K., Sharma, A. K., & Bhatia, S. K. (2023). Layered double hydroxides and their tailored hybrids/composites: Progressive trends for delivery of natural/synthetic-drug/cosmetic biomolecules. *Environmental Research*, *238*(Pt 2), 117171. https://doi.org/10.1016/j.envres.2023.117171

[7] Vuksanović, M. M., Egelja, A., Barudžija, T., Tomić, N., Petrović, M., Marinković, A., Radojević, V., & Heinemann, R. J. (2021). Inorganically modified particles FeAl-LDH@$SiO_2$ as reinforcement in poly (methyl) methacrylate matrix composite. *Royal Society Open Science*, *8*(9), 210835. https://doi.org/10.1098/rsos.210835

[8] Yu, S., Choi, G., & Choy, J.-H. (2023). Multifunctional layered double hydroxides for drug delivery and imaging. *Nanomaterials*, *13*(6), 1102. https://doi.org/10.3390/nano13061102

[9] Zhang, Y., Xu, H., & Lu, S. (2021). Preparation and application of layered double hydroxide nanosheets. *RSC Advances*, *11*(39), 24254–24281. https://doi.org/10.1039/d1ra03289e

[10] Rashed, S. H., Abd-Elhamid, A., Abdalkarim, S. Y. H., El-Sayed, R. H., El-Bardan, A. A., Soliman, H. M., & Nayl, A. (2022). Preparation and characterization of layered-double hydroxides decorated on graphene oxide for dye removal from aqueous solution. *Journal of Materials Research and Technology*, *17*, 2782–2795. https://doi.org/10.1016/j.jmrt.2022.02.040

[11] Raheem, S. A., & Mohammed, A. A. (2024). Synthesis, characterization, and applications of layered double hydroxides nanocomposites for the adsorption of organic and inorganic contaminants from an aqueous solution: An overview. *Results in Surfaces and Interfaces*, *18*, 100386. https://doi.org/10.1016/j.rsurfi.2024.100386

[12] Liu, Q., Fan, G., Zhang, S., Liu, Y., & Li, F. (2012). Synthesis of uniform Ni–Al layered double hydroxide via a novel reduction–oxidation route. *Materials Letters*, *82*, 4–6. https://doi.org/10.1016/j.matlet.2012.05.039

[13] Zhao, Y., Li, F., Zhang, R., Evans, D. G., & Duan, X. (2002). Preparation of layered double-hydroxide nanomaterials with a uniform crystallite size using a new method involving separate nucleation and aging steps. *Chemistry of Materials*, *14*(10), 4286–4291. https://doi.org/10.1021/cm020370h

[14] Klydziute, G., Gliaudyte, L., Sokol, D., Vasiliauskiene, D., Yang, T. C., & Kareiva, A. (2024). Layered double hydroxides: Sol-gel synthesis, characterization and application. *Research Square*. https://doi.org/10.21203/rs.3.rs-5346865/v1

[15] Jin, L., Sun, Y., Zhou, X., Wen, J., Wang, F., Ning, X., Wen, Y., Wu, D., & Peng, L. (2022). One-Step synthesis of layered double hydroxides by a Solvent-Free method. *ACS Sustainable Chemistry & Engineering*, *10*(39), 12955–12961. https://doi.org/10.1021/acssuschemeng.2c04436

[16] Gao, Z., Sasaki, K., & Qiu, X. (2018). Structural memory effect of Mg–Al and Zn–Al layered double hydroxides in the presence of different natural humic acids: Process and mechanism. *Langmuir*, *34*(19), 5386–5395. https://doi.org/10.1021/acs.langmuir.8b00059

[17] Singha Roy, A., Kesavan Pillai, S., & Ray, S. S. (2022). Layered double hydroxides for sustainable agriculture and environment: An overview. *ACS omega*, *7*(24), 20428–20440. https://doi.org/10.1021/acsomega.2c01405

[18] Kameliya, J., Verma, A., Dutta, P., Arora, C., Vyas, S., & Varma, R. S. (2023). Layered double hydroxide materials: A review on their preparation, characterization, and applications. *Inorganics*, *11*(3), 121. https://doi.org/10.3390/inorganics11030121

[19] Bhojaraj, & Rajamathi, M. (2023). Anion Exchange Reactions of 3R2-MgAl-Carbonate-LDH: Comparison with the 3R1 analogue and formation of 3R2 polytype of MgAl-LDH with other interlayer anions. *ACS Omega*, *8*(11), 10185–10190. https://doi.org/10.1021/acsomega.2c07515

[20] Richardson, M. C., & Braterman, P. S. (2007). Infrared spectra of oriented and nonoriented layered double hydroxides in the range from 4000 to 250 $cm^{-1}$, with evidence for regular short-range order in a synthetic magnesium−aluminum LDH with Mg:Al = 2:1 but Not with Mg:Al = 3:1. *The Journal of Physical Chemistry C*, *111*(11), 4209–4215. https://doi.org/10.1021/jp064744w

[21] Zamaraite, I., Vieira, D. E. L., Vieira, L. G., Ribeiro, J. L., Vieira, J. M., Salak, A. N., & Banys, J. (2021). Dielectric and infrared spectroscopy characterization of Co–AL layered double hydroxides. *Physica Status Solidi (A)*, *218*(15). https://doi.org/10.1002/pssa.202100106

[22] Zhou, J., Ma, P., Li, C., Li, S., Li, C., Wu, F., & Dou, Y. (2026). Research Progress on Layered Double Hydroxides and Their Derivatives toward Solar-to-Chemical Energy Conversion. *ACS Applied Materials & Interfaces*, *18*(15), 21424–21443. https://doi.org/10.1021/acsami.6c00782

[23] Kaur, H., Singh, S., & Pal, B. (2021). A brief review on modified layered double hydroxides for H2 production through photoinduced H2O splitting. *Environmental Nanotechnology Monitoring & Management*, *16*, 100451. https://doi.org/10.1016/j.enmm.2021.100451

[24] Santos, M. F., Moraes, P. I. R., Tavares, S. R., Martins, A., Capaz, R. B., Wypych, F., & Leitão, A. A. (2025). Analysis of the energy and nature of bandgap in layered double hydroxides Mg-Al-X and Zn-Al-X (X= $Cl^-$, $OH^-$, $CO_3^{2-}$, or $NO_3^-$). *Applied Clay Science*, *279*, 108061. https://doi.org/10.1016/j.clay.2025.108061

[25] Saeed, M., Zafar, M., Razzaq, A., Khan, S. A., Khan, Z., & Kim, W. Y. (2022). Visible-light-active Zn–Fe layered double hydroxide (LDH) for the photocatalytic conversion of rice husk extract to value-added products. *Applied Sciences*, *12*(5), 2313. https://doi.org/10.3390/app12052313

[26] Bobde, P., Patel, R. K., Panchal, D., Sharma, A., Sharma, A. K., Dhodapkar, R. S., & Pal, S. (2021). Utilization of layered double hydroxides (LDHs) and their derivatives as photocatalysts for degradation of organic pollutants. *Environmental Science and Pollution Research*, *28*(42), 59551–59569. https://doi.org/10.1007/s11356-021-16296-x

[27] Mohapatra, L., & Parida, K. (2011). Zn–Cr layered double hydroxide: Visible light responsive photocatalyst for photocatalytic degradation of organic pollutants. *Separation and Purification Technology*, *91*, 73–80. https://doi.org/10.1016/j.seppur.2011.10.028